Two pion decay of the Roper resonance

E. Hernández,[1] E. Oset,[2] and M. J. Vicente Vacas[2]

[1]*Grupo de Física Nuclear, Facultad de Ciencias, Universidad de Salamanca, Plaza de la Merced s/n, 37008 Salamanca, Spain*
[2]*Departamento de Física Teórica e IFIC, Centro Mixto Universidad de Valencia-CSIC, Institutos de Investigación de Paterna,*
Apartado correos 22085, 46071 Valencia, Spain

We evaluate the two-pion decay of the Roper resonance in a model where explicit rescattering of the two final pions is accounted for by the use of unitarized chiral perturbation theory. Our model does not include an explicit ϵ or σ scalar-isoscalar meson decay mode; instead it generates it dynamically by means of the pion rescattering. The two ways, explicit or dynamically generated, of introducing this decay channel have very different amplitudes. Nevertheless, through interference with the other terms of the model, we are able to reproduce the same phenomenology as models with explicit consideration of the ϵ meson.

I. INTRODUCTION

The Roper resonance is one of the controversial resonances, with an abnormally large width comparative to other resonances with larger mass. It appears naturally in quark models with a radial excitation of one of the quarks [1–3], but it has also been suggested that it is dynamically generated by the meson-baryon interaction itself [4], and thus would be essentially formed by a large meson-nucleon cloud. One of the intriguing properties of the Roper is its two-pion decay mode. According to the Particle Data Group (PDG) [5], it has a 30–40 % branching ratio into $N\pi\pi$, mostly going to $\Delta\pi$, and a small fraction of 5–10 %, which goes into a nucleon and two pions in s wave and isospin, $I=0$. This scalar-isoscalar mode plays a very important role in all reactions involving two-pion production close to threshold. The reason is that the contribution from the nucleon intermediate states cancels at threshold when the direct and crossed terms are taken into account. Then the next resonance, which is the Δ, involves p-wave couplings which would vanish at threshold, and finally comes the Roper resonance that, thanks to this nonvanishing scalar-isoscalar decay mode into two pions, gives a nonvanishing contribution to the threshold amplitudes. This has been shown explicitly to be the case in pion-induced two-pion production [6–9], photon-induced two-pion production [10,11], and two-pion production in nucleon-nucleon collisions [12–15]. The influence of the Roper excitation and its decay modes in many other reactions has been discussed in Refs. [16–18]. Similarly, it has also been shown [19,20] in the study of the Roper excitation in the (α, α') reaction that the Roper is very efficiently excited by an isoscalar source, which should somehow be related to this scalar-isoscalar decay.

The evidence for this scalar-isoscalar two-pion decay comes mostly from the analysis of Manley and co-workers [21,22], where he fits the data by means of the excitation of an ϵ meson of about 800 MeV mass and width plus the decay into $\Delta\pi$. This ϵ meson is what we would call now the σ meson, or in an alternative nomenclature, the $f_0(400–900)$ meson, as also used by the PDG. However, the immediate conceptual problem arises, since, whatever this meson is called, the strength of the two-pion distribution does not follow the shape provided by the exchange of such a heavy and broad meson. The isoscalar two-pion distribution at low energies is governed by the scattering matrix of two pions in $L=0, I=0$, which has a broad bump consisting of a large background on top of the effects of the σ pole, which is now present in all modern theoretical [23–25] and experimental analyses [26,27] (see also the proceedings of the σ workshop [28]). The pole of the σ appears in all these approaches with a mass around 500 MeV and a width around 400 MeV, and as mentioned above, there is also a large background present in the $\pi\pi$ t matrix.

In the present context it is also worth mentioning that the use of chiral perturbation theory [29] and its unitary extensions in coupled channels [23,24,30–34] has brought a new perspective on the nature of the scalar meson resonances, particularly the σ. Indeed, what is found in these works is that the σ is generated dynamically from the lowest-order chiral Lagrangian and the multiple scattering of the mesons implicit in the unitary approach. This finding and the previous statement are more than semantics, because it implies that anything associated with the production of a σ should be considered as the production of two pions that undergo final-state interaction (in this case in the strong $L=0, I=0$ channel). This is the philosophy taken in the present work, where we perform a theoretical study of the two-pion decay of the Roper, with the explicit consideration of the final-state interaction of the two pions, which automatically generates the production of this two-pion σ mode. The approach is hence different from the one followed in Refs. [21,22] since we do not allow the direct production of a σ. Yet, we aim at reproducing the same phenomenology that was fitted in the analysis of Refs. [21,22]. We will show how this is possible, and even if a very different, and obviously more realistic, distribution of the two-pion invariant mass is obtained for the scalar isoscalar decay mode, the coherent sum of the different mechanisms that we have leads to mass distributions of the two pions or of one pion-nucleon system, in agreement with the results that one would obtain with Manley's approach of $\Delta\pi$ plus the massive and broad ϵ meson production.
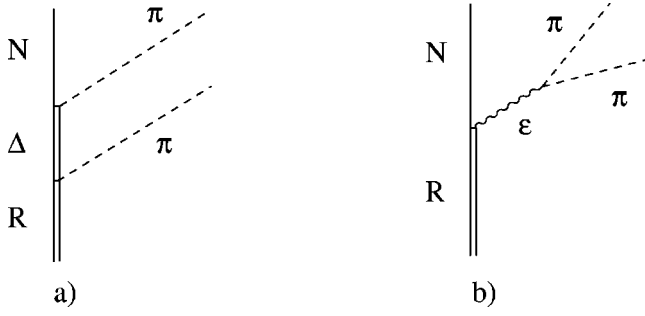
FIG. 1. Feynman diagrams for the two processes contributing to the Roper decay into two pions in Manley's approach. (a) $\Delta\pi$ intermediate channel. (b) $N\epsilon$ intermediate channel.

II. MANLEY'S APPROACH FOR THE TWO-PION DECAY OF THE ROPER

In this section we will translate the two-pion decay model of the Roper described in Refs. [21,22] to the language of Lagrangian and Feynman diagrams. As explained in the Introduction, the model has two intermediate decay channels for the Roper decay into two pions: the Roper decay can take place either into an intermediate $\Delta\pi$ state or into an intermediate $N\epsilon$ state. The ϵ meson is a scalar-isoscalar meson with a mass and width of $M_\epsilon = \Gamma_\epsilon(M_\epsilon) = 800$ MeV. The Feynman diagrams for the two decaying modes appear in Figs. 1(a) and 1(b). In the spirit of Refs. [21,22], we will use here nonrelativistic Lagrangian for the different vertices involved in the calculation. Those Lagrangian are given, with obvious notation, as

$$\mathcal{L}_{R\Delta\pi}(x) = \frac{f_{R\Delta\pi}}{m_\pi} \Psi_\Delta^\dagger(x) S_j^\dagger \mathbf{T}^\dagger [\partial_j \boldsymbol{\pi}(x)] \Psi_R(x) \epsilon(x),$$

$$\mathcal{L}_{\Delta N\pi}(x) = \frac{f_{\Delta N\pi}}{m_\pi} \Psi_N^\dagger(x) S_j \mathbf{T} [\partial_j \boldsymbol{\pi}(x)] \Psi_\Delta(x), \quad (1)$$

and

$$\mathcal{L}_{RN\epsilon}(x) = g_{RN\epsilon} \Psi_N^\dagger(x) \Psi_R(x) \epsilon(x),$$

$$\mathcal{L}_{\epsilon\pi\pi}(x) = g_{\epsilon\pi\pi} \epsilon(x) \boldsymbol{\pi}(x) \boldsymbol{\pi}(x). \quad (2)$$

$S^\dagger$ and $T^\dagger$ are, respectively, the spin and isospin operators for the $1/2$ to $3/2$ transition, with matrix elements just given by Clebsch-Gordan coefficients.

The amplitude for the process in Fig. 1(a) is given by

$$\mathcal{M}_{1a} = i \frac{f_{R\Delta\pi}}{m_\pi} \frac{f_{\Delta N\pi}}{m_\pi} \Phi_N^\dagger \chi_N^\dagger \left[\left(\frac{2}{3} \mathbf{q}_1 \cdot \mathbf{q}_2 - \frac{i}{3} \boldsymbol{\sigma} \cdot (\mathbf{q}_1 \times \mathbf{q}_2) \right) \right.$$

$$\times \left(\frac{2}{3} \delta_{j_1 j_2} - \frac{i}{3} \varepsilon_{j_1 j_2 k} \cdot \boldsymbol{\tau}_k \right) \frac{M_\Delta}{E_\Delta(\mathbf{q}_1)}$$

$$\times \frac{1}{M_R - q_1^0 - E_\Delta(\mathbf{q}_1) + \frac{i}{2}\Gamma_\Delta(p_R - q_1)} + (1 \leftrightarrow 2) \right]$$

$$\times \Phi_R \chi_R. \quad (3)$$

Φ and χ are, respectively, isospin and spin Pauli spinors for both the nucleon and the Roper while $\boldsymbol{\tau}$ and $\boldsymbol{\sigma}$ are the isospin and spin Pauli matrices. $p_R = (M_R, \mathbf{0})$, q_1 and q_2 are the four-momentum of the Roper and the two pions, and $E_\Delta(\mathbf{q})$ is the on-shell energy of a Δ with three-momentum $\mathbf{q}$. Finally j_1 and j_2 are isospin indices in the Cartesian base for the two pions. Note that since we are working in the isospin mathematical base, the pions are identical particles and the amplitude has to be symmetrized with respect to the exchange of the pions. In the expression for the width, we have to include a factor $1/2$ of symmetry. For the process in Fig. 1(b), we get

$$\mathcal{M}_{1b} = -2i g_{RN\epsilon} g_{\epsilon\pi\pi} \frac{1}{s - M_\epsilon^2 + i M_\epsilon \Gamma_\epsilon(s)}$$

$$\times \Phi_N^\dagger \cdot \Phi_R \chi_N^\dagger \cdot \chi_R \delta_{j_1 j_2}, \quad (4)$$

where s is the total four-momentum square of the two final pions. Even though the previous amplitudes are nonrelativistic for the phase space integrals, we shall take into account all the appropriate relativistic factors. As for the coupling constants, we fix $f_{\Delta N\pi}$ from the width of the Δ as given by the PDG. A value of $f_{\Delta N\pi} = 2.07$ results. For the other coupling constants, one needs information on the width of the Roper associated to the two channels involved. Those values and the mass of the Roper we take from Manley's analysis. Comparing $\Gamma_{R \to \Delta\pi} = 88$ MeV to the result obtained with the use of the Feynman diagram of Fig. 1(a), one gets $f_{R\Delta\pi} = 1.56$, while from $\Gamma_{R \to N\epsilon} = 33$ MeV and the evaluation of the contribution due to the Feynman diagram in Fig. 1(b), one determines the product of coupling constants $g_{RN\epsilon} \cdot g_{\epsilon\pi\pi} = (1.43 \times 10^{-2}) M_\epsilon^2$ MeV^{-1}. The sign of this product of coupling constants relative to $f_{R\Delta\pi}$ is chosen to be positive in accordance with the sign assignment done in Ref. [22]. Note also that for the first process, the pions can be in both $I = 0,1$ isospin states while for the second, only $I = 0$ is allowed. The total width for the Roper decay into two pions that we get when taking into account both terms is given by $\Gamma_{R \to N\pi\pi} = 153$ MeV, meaning that there is constructive interference between the two contributions. While this interference effect is also present in the amplitude used in Ref. [22] there the total width is taken to be $\Gamma_{R \to N\pi\pi} = \Gamma_{R \to \Delta\pi} + \Gamma_{R \to N\epsilon} = 121$ MeV.

In Fig. 2 we give two-pion invariant mass distributions obtained within the approach just described. The distribution that arises from considering the intermediate channel $N\epsilon$ alone is represented by the dotted line, and it is essentially given by phase space. The dashed line gives now the distribution corresponding to the intermediate $\Delta\pi$ state. There one sees two peaks at large and small invariant masses, which are due to the presence of a $(\vec{q}_1 \cdot \vec{q}_2)^2$ term, with $\vec{q}_{1,2}$ the three-momentum of the pions, in the amplitude square [see Eq. (3)]. The maximum for this quantity is reached when the two pions move in the same direction (small invariant mass) or in opposite direction (large invariant mass). The invariant mass distribution corresponding to the coherent sum of the two channels is given by the full curve. The
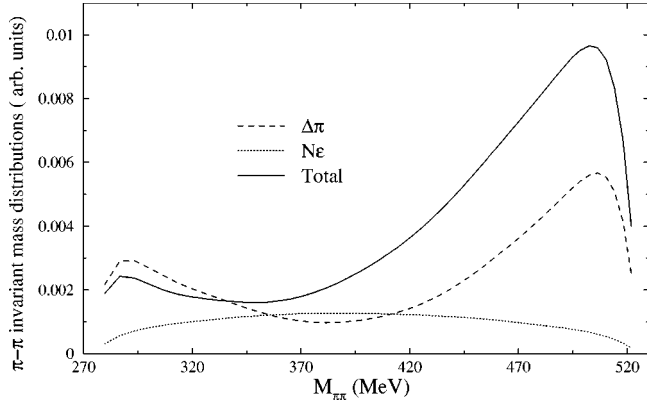
FIG. 2. π-π invariant mass distributions as obtained in Manley's approach. Dashed line: distribution obtained by considering the $\Delta\pi$ intermediate channel alone. Dotted line: distribution obtained by considering the $N\epsilon$ intermediate channel alone. Full curve: total result.

interference effect is clearly seen at large and small invariant masses. While the peak at large invariant mass increases, the one at low invariant mass decreases.

In Fig. 3 we show pion-nucleon invariant mass distributions. As before, the $N\epsilon$ contribution is basically given by phase space, while the $\Delta\pi$ one shows a peak below the Δ mass. In the total contribution, the central peak is enhanced due to interference.

As these invariant mass distributions are obtained from amplitudes that are fitted to experiment, we will consider them as if they were true "experimental results" to which we can compare our own results.

III. MODEL FOR THE TWO-PION DECAY OF THE ROPER

In our model we will consider two types of contributions. In the first type that we shall call open-diagram contribution, the Roper decays into a baryon and a pion and then the baryon decays into a nucleon and pion. No final-state interaction between the two pions is considered. For the intermediate baryon, we take Δ, nucleon, and Roper itself.

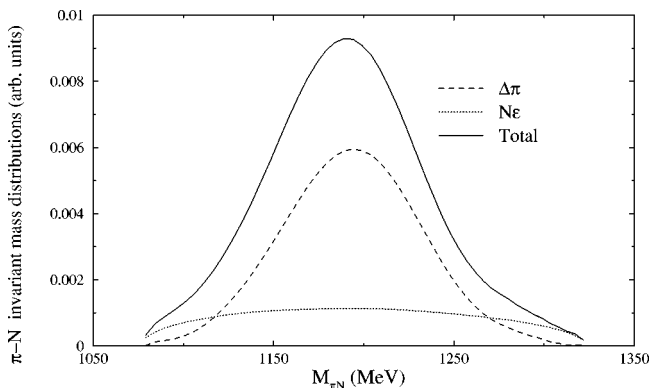This contribution, whose Feynman diagrams appear in

FIG. 3. π-N invariant mass distributions as obtained in Manley's approach. Notation as in Fig. 2.
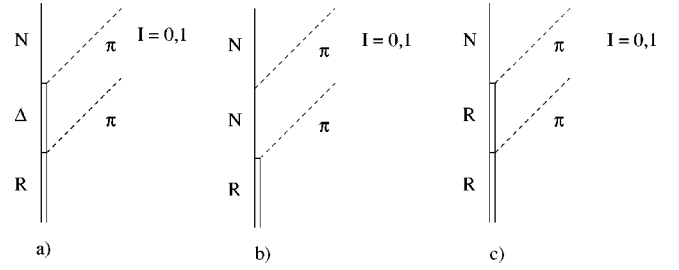

FIG. 4. Feynman diagrams corresponding to our "open diagrams" contribution to the Roper decay into two pions. Diagrams (a), (b), and (c) correspond to taking Δ, nucleon, or Roper as intermediate baryons. The two final pions can be in both $I=0,1$ isospin states.

Fig. 4, is the equivalent in our model of the $\Delta\pi$ intermediate channel in Manley's approach. The differences come from the fact that we include also $N\pi$ and $R\pi$ intermediate states and we take into account relativistic corrections for the vertices involved. Those relativistic corrections are given for the $N' \to N\pi$ transition as

$$\boldsymbol{\sigma}\cdot\mathbf{q} \to \boldsymbol{\sigma}\cdot\mathbf{q}\left(1 - \frac{q^0}{2M'}\right) - \boldsymbol{\sigma}\cdot\mathbf{p}\left(\frac{q^0}{2M'} + \frac{q^0}{2M}\right), \quad (5)$$

where N', N stand for either nucleon or Roper, $(q^0, \mathbf{q})$ is the pion four-momentum, and $\mathbf{p}$ the three-momentum of the final N. This comes automatically from the evaluation of the matrix elements of the $\gamma^\mu \gamma_5 \partial_\mu$ operator of the pseudovector coupling of the pions to the nucleons. For the vertices involving Δ, we take the Lagrangian of Eq. (1), where it has been implicitly assumed that Δ is at rest, and introduce the appropriate modification;

$$\mathbf{S}^\dagger \cdot \mathbf{q} \to \mathbf{S}^\dagger \cdot \left(\mathbf{q} - \frac{q^0}{M_\Delta}\mathbf{p}_\Delta\right),$$

$$\mathbf{S}\cdot\mathbf{q} \to \mathbf{S}\cdot\left(\mathbf{q} - \frac{q^0}{M_\Delta}\mathbf{p}_\Delta\right). \quad (6)$$

For the coupling constants we take $f_{NN\pi} = g_A(m_\pi/2f_\pi) = 0.95$, the naive quark model result $f_{RR\pi} = f_{NN\pi}$, and for $f_{RN\pi}$ we use the experimental information on $\Gamma_{R\to N\pi} = 270$ MeV, from which $f_{RN\pi} = 0.40$. We still have to fix $f_{R\Delta\pi}$.

For that we need our second type of contribution, which we call closed-diagram contribution, and that we do the construction by allowing the two pions in the final state to rescatter in the $I=0$ isospin channel. The corresponding Feynman diagrams appear in Fig. 5 and this is our model analog of the $N\epsilon$ channel in Manley's analysis.

To fully define our model we have to give the form factors that we use to regularize the loop integrals and also the $\pi\pi$ t matrix for the channel $L=0, I=0$. The latter will be given in the following section. For each of the baryon-baryon-pion vertices, we take a monopole form factor
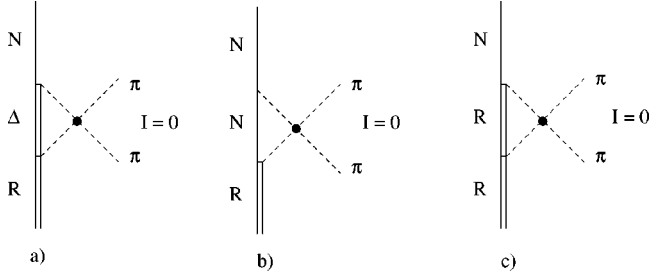
FIG. 5. Feynman diagrams corresponding to our "closed-diagram" contribution to the Roper decay into two pions. (a)–(c) as in Fig. 4. The big dot represents the $\pi\pi$ t matrix in the $I=0$ channel. Rescattering in the $I=1$ channel is neglected.

$$F(\mathbf{q}) = \frac{\Lambda^2}{\Lambda^2 + \mathbf{q}^2}, \tag{7}$$

with the same value of Λ for all cases. We will discuss the cutoff dependence in Sec. IV.

As an illustration we give the amplitude corresponding to the process in Fig. 5(a),

$$
\mathcal{M}_{5a} = \frac{2}{3\sqrt{3}} \frac{f_{R\Delta\pi}}{m_\pi} \frac{f_{\Delta N\pi}}{m_\pi} \Phi_N^\dagger \chi_N^\dagger \left(\int \frac{d^4 q}{(2\pi)^4} \left\{ \left[\left(\frac{2}{3} (\mathbf{p}_N - \mathbf{q}) \cdot \mathbf{q} \right) \right. \right. \right.
$$

$$
\left. - \frac{i}{3} \boldsymbol{\sigma} \cdot ((\mathbf{p}_N - \mathbf{q}) \times \mathbf{q}) \right) \left(1 + \frac{M_R}{M_\Delta} - \frac{q^0}{M_\Delta} \right)
$$

$$
+ \frac{2}{3} \mathbf{q}^2 \frac{q^0 - p_N^0}{M_\Delta} \left] \frac{M_\Delta}{E_\Delta(\mathbf{q})} \frac{1}{q^0 - E_\Delta(\mathbf{q}) + \frac{i}{2}\Gamma_\Delta(q)} \right.
$$

$$
\times \frac{1}{(p_N^0 - q^0)^2 - (\mathbf{p}_N - \mathbf{q})^2 - m_\pi^2 + i\varepsilon}
$$

$$
\times \frac{1}{(M_R - q^0)^2 - \mathbf{q}^2 - m_\pi^2 + i\varepsilon}
$$

$$
\left. \times \frac{\Lambda^2}{\Lambda^2 + (\mathbf{p}_N - \mathbf{q})^2} \frac{\Lambda^2}{\Lambda^2 + \mathbf{q}^2} \right\} t_{\pi\pi}^{I=0}(s) \right) \Phi_R \chi_R. \tag{8}
$$

Here q and p_N are, respectively, the four-momentum of the Δ in the loop and of the final nucleon. For the two final pions we have already taken into account the fact that they are in an $I=0$ isospin state. Similar results are obtained for the case of intermediate nucleon [Fig. 5(b)] or Roper [Fig. 5(c)]. All
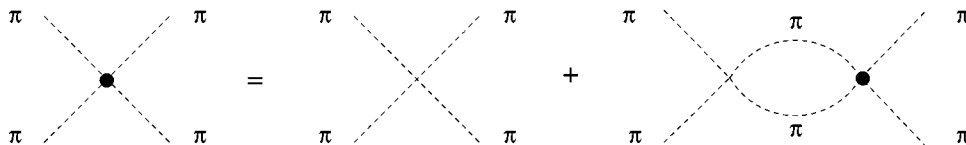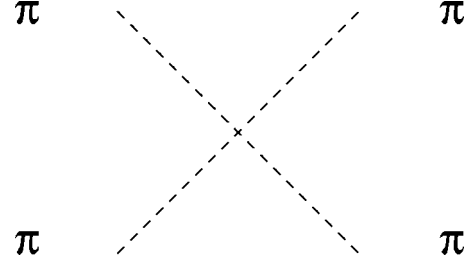

FIG. 6. Feynman diagram for the $\pi\pi$ potential.

baryon propagators that we use throughout the paper contain a momentum-dependent imaginary part. In all cases we use the expression for the width corresponding to the $N\pi$ decay channel. For the Roper we rescale that result to its total width.

We fix the $f_{R\Delta\pi}$ coupling constant by fitting with our full model, including the $\pi\pi$ t matrix given in the following section, the total Roper decay width into two pions. For this width we take $\Gamma_{R\rightarrow N\pi\pi} = 153$ MeV, as evaluated in the preceding section and obtain a coupling constant that depends on the cutoff Λ. The best agreement with the invariant mass distributions is obtained with $\Lambda = 0.7$ GeV, which gives $f_{R\Delta\pi} = 1.1$ to be compared to 1.56 obtained in Manley's approach. Larger Λ values as those used in Ref. [35] also agree reasonably with data.

$\pi\pi$ t matrix in the $L=0,I=0$ channel

The $\pi\pi$ t matrix in the $L=0,I=0$ channel we take from Refs. [23,24], where they use a nonperturbative approach that combines pion-pion potentials provided by the lowest-order chiral Lagrangian with the Lipmann-Schwinger equation. The pion-pion potential corresponding to Fig. 6 is given by

$$V_{\pi\pi}^{I=0} = -\frac{6}{f_\pi^2} \left(s - \frac{m_\pi^2}{2} - \frac{1}{3} \sum_j (q_j^2 - m_\pi^2) \right), \tag{9}$$

where $f_\pi = 92.4$ MeV is the pion decay constant and $\sqrt{s}$ gives the total energy in the center of mass. We give the potential separated into on-shell plus off-shell parts.

To obtain the t matrix, one sums an infinite set of diagrams where pions are allowed to rescatter in the s channel. Formally, one can write this Lipmann-Schwinger equation as

$$t_{\pi\pi}^{I=0} = V_{\pi\pi}^{I=0} + V_{\pi\pi}^{I=0} \cdot G \cdot t_{\pi\pi}^{I=0}, \tag{10}$$

where G stands for the loop in Fig. 7.

As shown in Ref. [23], the use of the off-shell part of the potential amounts to a renormalization of f_π and the pion

FIG. 7. Set of Feynman diagrams corresponding to the Lipmann-Schwinger equation used to evaluate the $\pi\pi$ t matrix in the $I=0$ channel. The contribution of kaons in the loop is neglected.

TABLE I. Contribution of the different mechanisms to the two-pion Roper decay width. All numbers are in MeV. "Δ alone" in our model results means that we consider the Δ as the only intermediate baryon. "No Δ" in our model results means that we take only nucleon and Roper as intermediate baryons. Note the constructive interference between the Δ alone and no Δ contributions in the closed-diagram case.

Our model		Manley's approach	
Open diagrams	55.3	$\Delta\pi$	88
Δ alone	54.7		
No Δ	0.6		
Closed diagrams	68.6	$N\epsilon$	33
Δ alone	31.8		
No Δ	8.2		
Coherent sum	153	Coherent sum	153

mass, and then it should not be included if one uses the physical values for those quantities. In that case Eq. (10) is purely algebraic and the factor G is given by

$$G(s=P^2) = \frac{i}{6}\int \frac{d^4q}{(2\pi)^4} \frac{1}{q^2-m_\pi^2+i\varepsilon} \frac{1}{(P-q)^2-m_\pi^2+i\varepsilon},$$
(11)

where P is the total four-momentum of the two incoming (outgoing) pions. The integral is divergent and has to be regularized. Here we follow Ref. [24] where dimensional regularization is used. The regularization mass that is treated in Ref. [24] as a free parameter is given by $\mu = 1.2$ GeV. The final expression for $G(s)$ is

$$G(s) = \frac{1}{6(4\pi)^2}\left(-1+\ln\frac{m_\pi^2}{\mu^2}+\sigma\ln\frac{\sigma+1}{\sigma-1}-i\pi\sigma\right),$$
(12)

where $\sigma = \sqrt{1-4m_\pi^2/s}$, and then

$$t_{\pi\pi}^{I=0} = -\frac{6}{f_\pi^2}\frac{s-m_\pi^2/2}{1+\frac{1}{f_\pi^2}(s-m_\pi^2/2)G(s)}.$$
(13)

We shall use this on-shell t matrix even though the two pions in the loop in Fig. 7 can be off shell. It has been shown in Ref. [35] that for the case of only nucleons and Δ's involved, the dominant off-shell contribution is canceled exactly by considering, at the same order in the chiral counting, diagrams that contain vertices with one baryon line and three pions. By analogy, a three-pion vertex involving the Roper should also be included to produce this cancellation in the Roper case. Hence, as in Ref. [35], we shall only take the on-shell part of the $\pi\pi$ interaction.

IV. RESULTS AND DISCUSSION

In Table I we show the contribution to the Roper decay width into two pions of our open- and closed-diagram
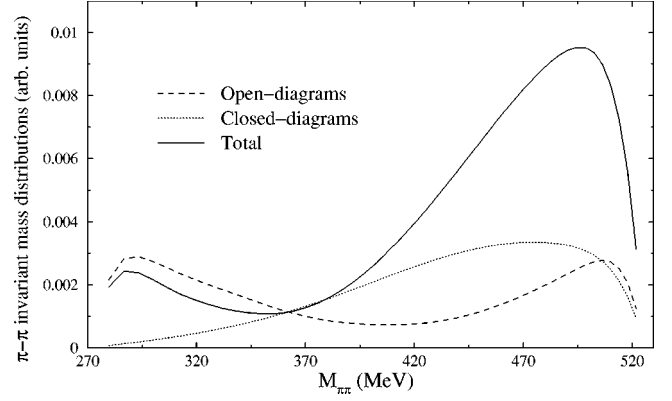

FIG. 8. π-π invariant mass distributions as obtained in our model. Dashed line: distribution obtained from considering the open-diagram contribution alone. Dotted line: distribution obtained from considering the closed-diagram contribution alone. Full curve: total result.

mechanisms for $\Lambda = 0.7$ GeV. Unless otherwise indicated, all results correspond to this cutoff value. The results that we obtain are compared to the contributions of the equivalent $\Delta\pi$ and $N\epsilon$ mechanisms in Manley's approach. The role of the mechanisms is different in the two models. While in Manley's approach the dominant contribution comes from the $\Delta\pi$ mechanism in our case the closed-diagram contribution, whose analog in Manley's analysis is the $N\epsilon$ channel, is larger. Also from the numbers in Table I, one sees that in our model the largest contribution to the width comes from considering the Δ to be the intermediate baryon. The contribution that comes from considering intermediate nucleon and Roper is very small and only for the case of closed diagrams the interference with the dominant intermediate Δ contribution is of some relevance.

In Fig. 8 we show now the two-pion invariant mass distribution obtained in our model. The dashed line corresponds to the open-diagram contribution. One sees the two-peak structure associated with the presence of the Δ. Compared to the $\Delta\pi$ distribution in Manley's approach we see that the peak at high invariant mass is reduced in our case. This is due to the relativistic corrections present in our model. The dotted line corresponds to the closed-diagram contribution. It has a broad peak at high invariant mass while it goes to zero at low invariant mass. Its shape is totally different from the phase space shape of the corresponding $N\epsilon$ contribution in Manley's analysis. These differences notwithstanding, we see that the distribution that corresponds to the coherent sum of the two channels resembles very much what one gets in Manley's approach. The two total distributions are compared now in Fig. 9 where one sees a good agreement between the two different approaches. Also in Fig. 9 we show the results for other values of the cutoff. This gives an idea of the theoretical uncertainties in our calculation.

A similar result is obtained for the pion-nucleon invariant mass distributions depicted in Fig. 10. The dashed line gives again the distribution corresponding to our open-diagrams mechanism. A peak is clearly seen around the Δ mass. The distribution corresponding to our closed-diagram mechanism
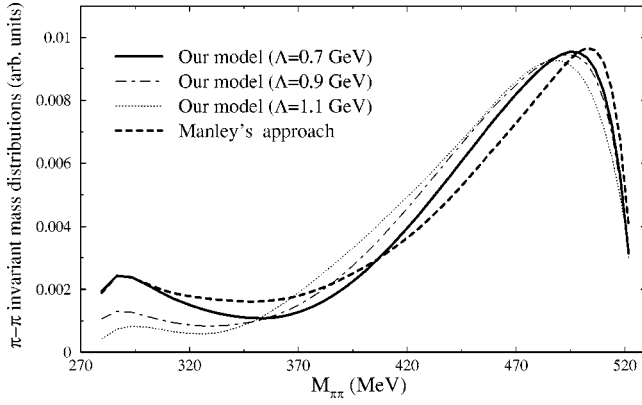
FIG. 9. Comparison of the π-π invariant mass distributions as obtained in the two models. Dashed line: Manley's approach distribution. Our model result: with $\Lambda = 0.7$ GeV ($f_{R\Delta\pi} = 1.1$) solid line, $\Lambda = 0.9$ GeV ($f_{R\Delta\pi} = 0.83$) dashed-dotted line, $\Lambda = 1.1$ GeV ($f_{R\Delta\pi} = 0.62$) dotted line.

is given by the dotted line. In this case its shape is closer to phase space. Both distributions are very different in magnitude from their corresponding $\Delta\pi$ and $N\epsilon$ in Manley's approach. But once again the coherent sum of both gives a result close to Manley's as can be seen in Fig. 11.

Our model is then able to reproduce the same phenomenology as Manley's approach without the need of an explicit $R \rightarrow N\epsilon$ coupling. This ϵ or σ meson is generated dynamically in our model through the rescattering of the final pions in the appropriate channel. Even though our open- and closed-diagram contributions and their counterparts, $\Delta\pi$ and $N\epsilon$ channels, in Manley's analysis are individually quite different, we have seen that the total result is very close in both models due to interference.

Extrapolation to low invariant masses

In this section we extrapolate our model to low invariant mass for the Roper. This region for the Roper invariant mass is explored when studying two-pion production close to threshold in nucleon-nucleon collisions. It is known that for the case where the two final pions are in an isospin $I = 0$ state, a phenomenological two-pion s-wave coupling of the type
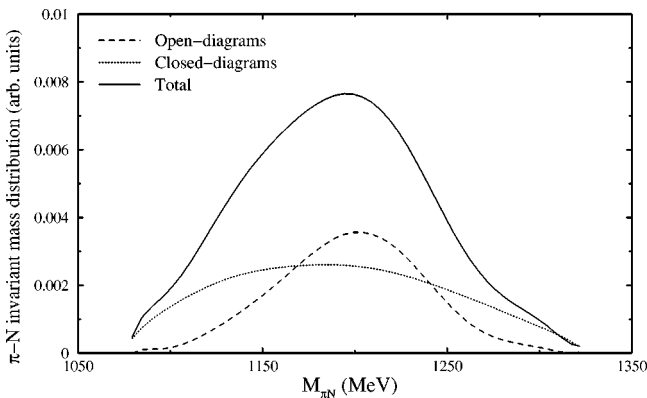

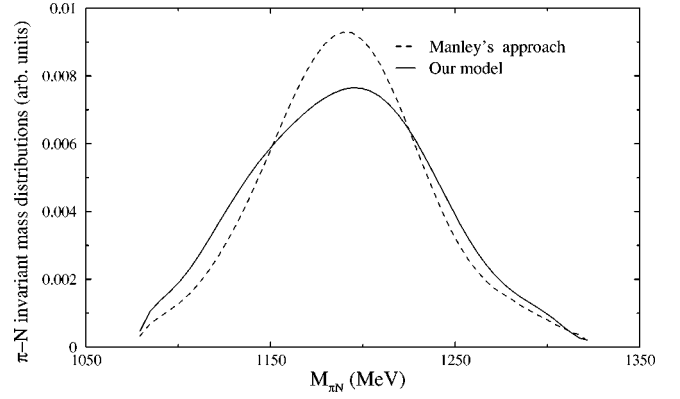FIG. 10. π-N invariant mass distributions as obtained in our model. Notation as in Fig. 8.

$$\mathcal{L}_{RN\pi\pi} = g_{RN\pi\pi} \Psi_N^\dagger(x) \Psi_R(x) \boldsymbol{\pi}(x) \cdot \boldsymbol{\pi}(x), \quad (14)$$

with $g_{RN\pi\pi} \simeq 1.6 \times 10^{-2}$ MeV^{-1} is able to explain the experimental data [12]. The use of this phenomenological term was suggested by the Roper decay into nucleon plus two s-wave pions. The value of the coupling constant in Ref. [12] was fitted to the Roper decay width into $N(\pi\pi)_{S-wave}^{I=0}$ using for that the central values given by the PDG [36].

Using our model we have evaluated the two-pion decay width of the Roper for an invariant mass of the latter given by $M = 1218$ MeV, just slightly above the two-pion decay threshold. The contribution coming from our open diagrams is negligible as it should. The results obtained with our closed diagrams are collected in Table II.

At such a small invariant mass there is almost no momentum dependence left on the amplitude. We can extract an effective coupling constant to be compared to the one defined in Eq. (14). The value that we get is

$$g_{eff}^{Our-model} = (6.5 + i2.0)10^{-3} \text{ MeV}^{-1}, \quad (15)$$

its imaginary part coming from the physical cut where the intermediate nucleon and one of the pions appear on shell. The main difference is anyway in its module as

$$\frac{|g_{eff}^{Our-model}|}{g_{RN\pi\pi}} = 0.42. \quad (16)$$

This means that our model will underpredict the $L = 0, I = 0$ two-pion production cross sections close to threshold. In contrast with our result, Manley's approach will give an effective coupling of $g_{eff}^{Manley} \simeq 1.43 \times 10^{-2}$ MeV^{-1}, in agree-

TABLE II. Contribution of the closed-diagram mechanisms to the two-pion decay width of the Roper for invariant mass $M = 1218$ MeV. All numbers are in MeV. Notation as in Table I.

Our model	
Closed diagrams	1.1×10^{-3}
Δ alone	3.2×10^{-4}
No Δ	2.8×10^{-4}

ment with phenomenology. Our more fundamental model is able to reproduce Manley's results at the Roper mass but it clearly lacks some extra contribution at low invariant masses. It is clear that other mechanisms that would contribute to the small amplitude at threshold are missing, which however, would not significantly contribute in the Roper region where the Δ intermediate states give practically all the strength. Yet, it is still remarkable that the mechanisms that we have evaluated provide the dominant contribution over such a large span of energies.

V. CONCLUSIONS

We have developed a model for the the two-pion decay of the Roper where we take into account the rescattering of the two final pions by means of the use of unitarized chiral theory. The aim was to see if one could explain at a more fundamental level the need for the phenomenological decay channel $R \to N\epsilon$ introduced by Manley and co-workers in their analyses. Even though the two models have clear dif-

ferences, we have shown that we are able to reproduce the same phenomenology when working at the Roper mass.

Our model seems, nevertheless, to fail at low invariant masses for the Roper, indicating that we still lack some extra contributions. Work in this direction plus also work in the direction of obtaining microscopically a description of the $NN \to NN^*$ transition obtained in Ref. [20] from the data of Ref. [19] would be a natural continuation of the present work, complementing from the chiral symmetry perspective the work already done using quark models in Ref. [37].

[1] S. Capstick and W. Roberts, Phys. Rev. D **49**, 4570 (1994).

[2] F. Cano and P. González, Phys. Lett. B **431**, 270 (1998).

[3] R. Bijker, F. Iachello, and A. Leviatan, Ann. Phys. (N.Y.) **236**, 69 (1994).

[4] O. Krehl, C. Hanhart, C. Krewald, and J. Speth, Phys. Rev. C **62**, 025207 (2000).

[5] Particle Data Group, D. E. Groom *et al.*, Eur. Phys. J. C **15**, 1 (2000).

[6] E. Oset and M. J. Vicente-Vacas, Nucl. Phys. **A446**, 584 (1985).

[7] V. Sossi, N. Fazel, R. R. Johnson, and M. J. Vicente-Vacas, Phys. Lett. B **298**, 287 (1993).

[8] V. Bernard, N. Kaiser, and U. G. Meissner, Nucl. Phys. **B457**, 147 (1995).

[9] T. S. Jensen and A. F. Miranda, Phys. Rev. C **55**, 1039 (1997).

[10] J. A. Gómez Tejedor and E. Oset, Nucl. Phys. **A571**, 667 (1994).

[11] J. A. Gómez Tejedor and E. Oset, Nucl. Phys. **A600**, 413 (1996).

[12] L. Alvarez-Ruso, E. Oset, and E. Hernández, Nucl. Phys. **A633**, 519 (1998).

[13] L. Alvarez-Ruso, Phys. Lett. B **452**, 207 (1999).

[14] L. Alvarez-Ruso, Nucl. Phys. **A684**, 443 (2001).

[15] W. Brodowski *et al.*, Phys. Rev. Lett. **88**, 192301 (2002); H. Clement, in *Proceedings of the QNP 2002*, edited by J. Speth, Ch. Elster, and Th. Walcher [Eur. Phys. J. A (to be published)]; B. Hoistad, *Proceedings of the PANIC 2002* [Nucl. Phys. A (to be published)].

[16] M. Soyeur, Acta Phys. Pol. B **31**, 239 (2000).

[17] M. Soyeur, Acta Phys. Pol. B **29**, 2501 (1998).

[18] M. Soyeur, Nucl. Phys. **A671**, 532 (2000).

[19] H. P. Morsch *et al.*, Phys. Rev. Lett. **69**, 1336 (1992).

[20] S. Hirenzaki, P. Fernández de Cordoba, and E. Oset, Phys. Rev. C **53**, 277 (1996).

[21] D. M. Manley, R. A. Arndt, Y. Goradia, and V. L. Teplitz, Phys. Rev. D **30**, 904 (1984).

[22] D. M. Manley and E. M. Saleski, Phys. Rev. D **45**, 4002 (1992).

[23] J. A. Oller and E. Oset, Nucl. Phys. **A620**, 438 (1997); **A652**, 407(E) (1997).

[24] J. A. Oller, E. Oset, and J. R. Peláez, Phys. Rev. Lett. **80**, 3452 (1998); Phys. Rev. D **59**, 074001 (1999).

[25] G. Colangelo, J. Gasser, and H. Leutwyler, Nucl. Phys. **B603**, 125 (2001).

[26] M. Ishida, S. Ishida, T. Komada, and S. I. Matsumoto, Phys. Lett. B **518**, 47 (2001).

[27] R. Kaminski, L. Lesniak, and B. Loiseau, Eur. Phys. J. C **9**, 141 (1999).

[28] *Proceedings of the Workshop on the Possible Existence of the σ Meson and its Implication in Hadron Physics, Kyoto, 2000*, edited by S. Ishida *et al.* (KEK Proceedings, Kyoto, 2000), pp. 224–231. See webpage http://amaterasu.kek.jp/YITPws/

[29] J. Gasser and H. Leutwyler, Nucl. Phys. **B250**, 517 (1985).

[30] J. A. Oller and E. Oset, Phys. Rev. D **60**, 074023 (1999).

[31] N. Kaiser, Eur. Phys. J. A **3**, 307 (1998).

[32] J. Nieves and E. Ruiz Arriola, Phys. Lett. B **455**, 30 (1999).

[33] J. Nieves and E. Ruiz Arriola, Nucl. Phys. **A679**, 57 (2000).

[34] V. E. Markushin, Eur. Phys. J. A **8**, 389 (2000).

[35] E. Oset, H. Toki, M. Mizobe, and T. T. Takahashi, Prog. Theor. Phys. **103**, 351 (2000).

[36] R. M. Barnett *et al.*, Phys. Rev. D **54**, 1 (1996).

[37] B. Juliá-Díaz, A. Valcarce, P. González, and F. Fernández, Phys. Rev. C **66**, 024005 (2002).